Adv. Sci. Res., 14, 157–162, 2017
https://doi.org/10.5194/asr-14-157-2017

Advances in Science & Research
Open Access Proceedings

16th EMS Annual Meeting & 11th European Conference on Applied Climatology (ECAC)

GPS – Zenith Total Delay assimilation in different resolution simulations of a heavy precipitation event over southern France

Alberto Caldas-Álvarez[1], **Samiro Khodayar**[1], **and Olivier Bock**[2]

[1]Institute of Meteorology and Climate Research (IMK-TRO), Karlsruhe Institute of Technology (KIT), Karlsruhe, 76344, Germany
[2]IGN LAREG, Univ Paris Diderot, Sorbonne Paris Cité, 5 rue Thomas Mann, 75205 Paris CEDEX 13, France

Correspondence to: Alberto Caldas-Álvarez (alberto.caldas-alvarez@kit.edu)

Received: 15 January 2017 – Revised: 24 April 2017 – Accepted: 4 May 2017 – Published: 13 June 2017

Abstract. The aim of this study is to investigate the different pathways of the interaction between an improved atmospheric moisture distribution by Data Assimilation (DA) of Global Positioning System Zenith Total Delays (GPS-ZTD) on the simulation of a selected Heavy Precipitation Event (HPE) across different model horizontal resolutions (7 km, 2.8 km and 500 m). The initiation and evolution of deep moist convection and heavy precipitation taking place on the 24 September 2012, which had a dedicated Intensive Observation Period (IOP6) during the Hydrological cycle in the Mediterranean eXperiment (HyMeX) Special Observation period 1, are analysed. The results show an improvement in the representation of the Integrated Water Vapour (IWV) spatial distribution and temporal evolution when the data assimilation is applied as well as through the refinement of the model grids. However, important discrepancies between the simulated and the observed vertical profiles of humidity still remain after the DA, thus affecting the representation of convection and heavy precipitation. For the presented case study, the model simulations exhibited a wet bias. The assimilation entailed a drying of the low to middle troposphere over the study region during the 6 h prior to the storm initiation for every horizontal resolution. This reduced the instability present at the moment of storm initiation, weakening in return the intensity of convection and the number of cells triggered. The improvement observed in the atmospheric moisture content and distribution was not followed by an improved precipitation representation closer to observations. This highlights the relevance of correctly distributing the assimilated IWV in the vertical direction in the models.

1 Introduction

The prediction of Heavy Precipitation Events (HPEs) that typically strike the western Mediterranean region by late summer (Lee et al., 2016; Davolio et al., 2016) is still a challenge for current Numerical Weather Prediction (NWP) models. Under a weak synoptic forcing, the location and time of the triggered convective cells is determined by mesoscale temperature and humidity inhomogeneities that define unstable regions prone to lifting. If in addition, sufficient moisture and a triggering mechanism are present, convection will take place. This major role of water vapour in convection was addressed in modelling studies where variations of $1\,\mathrm{g\,kg^{-1}}$ in specific humidity were able to make a difference between intense convection and its complete suppression (Crook, 1996). That is why the misrepresentation of the moisture distribution within the models is an identified source of error for heavy precipitation simulations. However, significant improvement can be gained by refining the horizontal resolution in the models (Hackenbruch et al., 2016) and through Data Assimilation (DA) of humidity measurements. In particular, DA of Global Positioning System-derived Zenith Total Delays (GPS-ZTD) has shown a positive impact in the prediction of strong precipitation (Boniface et al., 2009). The presented research work aims at investigating the pathways of the interaction between an improved atmospheric moisture distribution by DA of GPS-ZTD and precipitation in NWP simulations of a selected HPE across different grid spacings (7 km, 2.8 km and 500 m).

2 Methodology

The non-hydrostatic regional weather prediction model COnsortium for Small-scale MOdelling (COSMO; Schättler et al., 2013) in its version 5.1 has been used to reproduce a HPE that took place on the night of the 24 September 2012 over southern Europe. This event was characterized by large precipitation totals, measured at stations in the Cevennes-Avignon region (named A1 with max. of 100 mm day^{-1}), the Gulf of Genoa and the north eastern Alpine region (A2 – max. of 60 mm day^{-1}), and north eastern Italy (A3 – max. of 160 mm day^{-1}). In this study, only results on the convection evolution and heavy precipitation over southern France (region A1) are shown.

Convection was triggered over the affected regions as a result of mesoscale instability and the advection of an upper-level trough towards the west (Hally et al., 2014). An Intensive Observation Period (IOP6) was dedicated to the study of this HPE in the framework of the Hydrological cycle in the Mediterranean Experiment (HyMeX; Ducrocq et al., 2014). The COSMO simulations span three days (22 September 2012 at 00:00 to 25 September 2012 at 00:00 UTC). Two approaches are applied in order to gain an improved representation of the humidity fields and its related impact on convection. On the one hand, a dense state-of-art GPS-derived ZTD data set (Fig. 1) is continuously assimilated during the three-day simulation period with a frequency of 10 min. This data set is provided by the Institut National de L'Information Géographique et Forestière (IGN; Bock et al., 2016) and has been specially homogenized for 25 European GPS networks as a contribution to the HyMeX community. Therefore, simulations (hereafter referred to as AS) are obtained by assimilating only GPS-ZTD data by means of the Nudging towards observations method (Schraff and Hess, 2012) using the operational nudging parameters employed at the German Weather Service (DWD). These, are compared to control runs (CTRL), with no assimilation of any type of observation. The second approach aims at obtaining an improved moisture representation through refining the model spatial resolution. To this end, the event is represented on three different grid spacings (7 km, 2.8 km and 500 m) in a nested configuration (simulation domains in Fig. 1). The simulations on the 7 km grid are forced using analysis data from the Integrated Forecasting System (IFS) of the European Centre for Medium-range Weather Forecasts (ECMWF) with a horizontal resolution of 18 km. Settings close to the operational COSMO-EU set up employed at the German Weather Service (DWD), including a convection parametrization scheme following the mass-flux Tiedtke type (Tiedtke, 1989), is used on a 40 level model configuration with an integration time of 60 s. The 2.8 km runs are

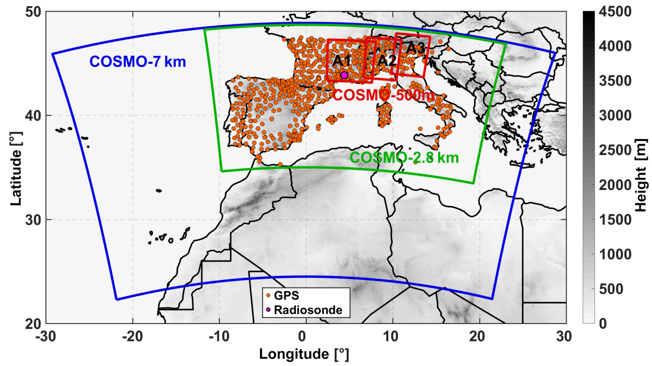

Figure 1. The 7 km, 2.8 km and 500 m simulation regions are denoted by the blue, green and red frames respectively. The GPS stations location is denoted by the orange dots and the location of the shown radiosonde measurement (see Fig. 3b) is indicated by the purple dot.

forced by the 7 km forecast runs, and the COSMO-DE configuration with 50 model levels and a time step for integration of 20 s was utilized. The deep convection parametrization scheme is not applied in this COSMO-DE configuration. Finally, specific settings for simulations in the lower limit of the mesoscale, including no convection parameterization and the use of a 3-D closure scheme for vertical turbulent diffusion (Doms et al., 2011) are used for the 500 m simulations. For this type of horizontal resolution the forcing data were obtained from the forecast runs of the 2.8 km grid model output, the number of atmospheric levels is 80 and the integration time step is 2 s. The external parameters of every simulation include orography data obtained from the Global Land One-km Base Elevation (GLOBE) Digital Elevation Model (Hastings et al., 2000). The Integrated Water Vapour (IWV) data set used for comparison of our model results against observations is also provided by the IGN and was derived from the ZTD data, employing surface pressure operational analysis from the AROME model in its west-Mediterranean configuration (AWMED) and the mean temperature computed from ERA-Interim pressure-level data following the algorithm described in Bevis et al. (1992). The rain gauges precipitation data set and the radiosonde profile shown in Sect. 3 are provided by the data base of HyMeX.

3 Results

3.1 Atmospheric moisture spatial distribution

Figure 2 represents the differences in the 24-hourly averaged IWV between observations (GPS-derived IWV) and the values simulated by COSMO at different horizontal resolutions. The nearest COSMO grid points to the stations location are chosen for the differences. Investigation area A1 is shown on the day prior to the storm initiation, the 23 September 2012, starting at 00:00 UTC. All CTRL runs show an

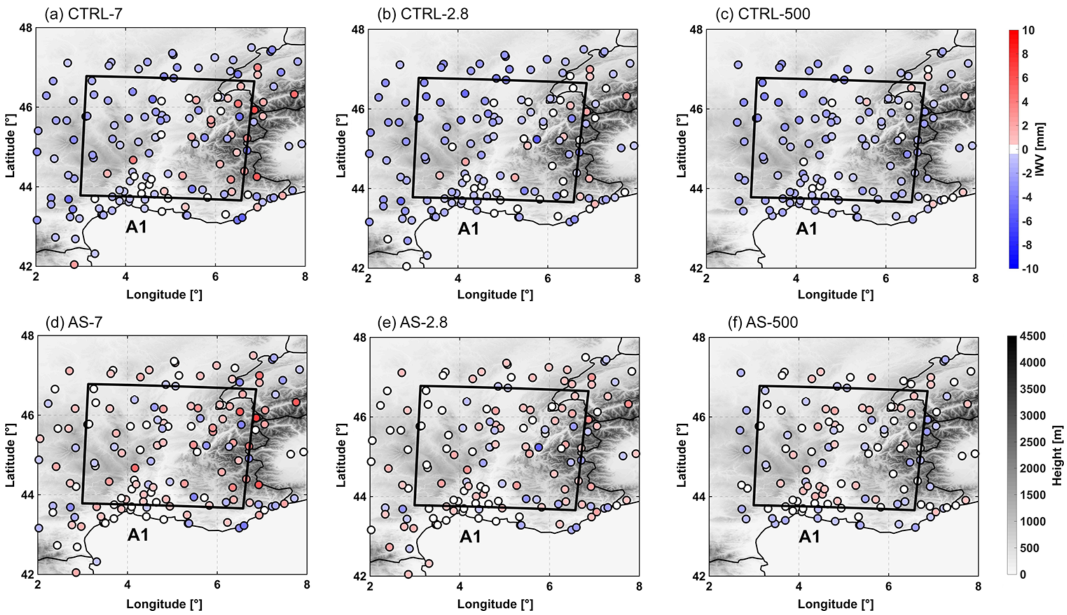

Figure 2. Spatial distribution of the 24-Hourly averaged IWV differences (GPS – COSMO). On the 23 September 2012 starting at 00:00 UTC.

overestimation of IWV by COSMO over the mountain regions in the western part of the study area, as well as through the Avignon valley reaching Lyon and the coast of the Gulf of Lion. This generalized wet bias is stronger in the CTRL-7 and CTRL-2.8 simulations in the northern part of the valley and over the upper left corner of the simulation region as compared to the CTRL-500. Nevertheless, over the Gulf of Lion, south to area A1, the CTRL-500 run represents a larger area of overestimation as compared to the CTRL-7 and CTRL-2.8 runs. Over the windward slope of the Alps, and the oriental flank of the Massif Central the CTRL-2.8 and the CTRL-7 runs exhibit singular locations with a large underestimation of the IWV values, not seen in the CTRL-500 runs. The general wet bias in the model results are reduced as a consequence of the assimilation for every model horizontal resolution. The mean of the IWV differences for the stations within area A1 is reduced from −0.6 mm (CTRL-7) to 0.5 mm (AS-7), from −1.3 mm (CTRL-2.8) to 0.1 mm (AS-2.8) and from −1.4 mm (CTRL-500) to 0.01 mm (AS-500). This is in agreement with the decrease in IWV seen in Fig. 2 over the mountain system and along the valley, however, the wet bias over the Gulf of Lion coast remains in the AS-500 runs. This is probably due to the proximity of the model boundaries that prevent any influence of the assimilation on moist advected air masses coming from regions south to the Gulf of Lion.

Figure 3a represents the temporal evolution of the IWV for the set of model simulations and the GPS-derived IWV measurements at a selected site (see Fig. 1). Discrepancies up to ca. 4 mm are found between the simulated and the measured IWV for every different CTRL run (7 km, 2.8 km and 500 m). As expected, the assimilation is able to correct these differences and its impact is strongest when the discrepancies between CTRL and the observations are largest. Such is the case on the 22 September 2012 at 02:00 UTC and during the 23 September 2012, between 08:00 and 18:00 UTC, most remarkably for the convection-permitting grids (AS-2.8 and CTRL-500). During the hours of convective precipitation three relative maxima of IWV are seen. The first maximum, within the precipitation time window (23 September 2012, 21:00 UTC to 24 September 2012, 10:00 UTC), is associated with the constant feeding of humidity, for at least 6 h prior to the arrival of the front by a south to south westerly flow. This increase is larger for the CTRL-2.8 and the CTRL-500 runs due to the advection of a more moist air mass originating at the Iberian Peninsula not seen in the AS-2.8, AS-500 runs neither in the CTRL-7 and AS-7 runs. The second maximum is associated to the arrival of the upper-level trough. Finally, the late increase in specific humidity at the 24 September 2012 09:00 UTC of about 1.5 mm for every model resolution is originated by the wake low of the front, enhanced in the AS runs as a result of the assimilation. Figure 3b shows the vertical profiles of temperature and dew point temperature of the set of simulations as well as measured by a radiosonde at the site (Fig. 1) on the 23 September at 12:00 UTC. Small differences in the temperature profiles exist between the CTRL simulations and their assimilated counterparts for every model resolution. The agreement with observations is usually good for this variable. The dew point temperature profiles are, however, strongly impacted by the assimilation. Between 08:00 and 18:00 UTC of 23 September 2012, the decrease in IWV in the AS runs caused by the

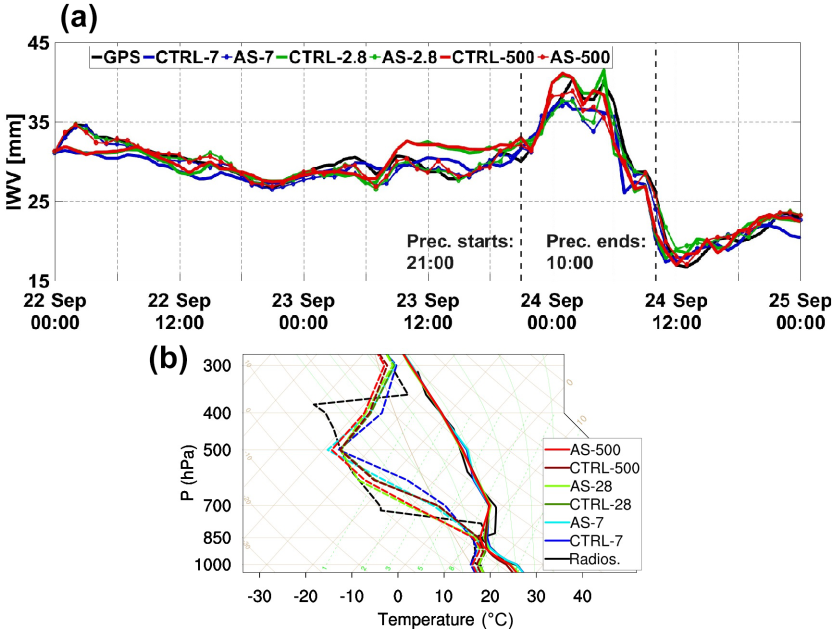

Figure 3. **(a)** Hourly IWV temporal evolution at a radiosonde site measured by the GPS and obtained with COSMO at the nearest grid points **(b)** Skew-T log at the same site on the 23 September 2012 at 12:00 UTC

assimilation is seen as a decrease in the mixing ratio between the 400 and 850 hPa levels, reaching differences even higher than 1 g kg^{-1}. Regarding the agreement with observations, important differences in the dew point temperature profile still remain after the assimilation. Figure 3b illustrates these existing discrepancies, with differences as large as 2 g kg^{-1} in the mixing ratio between the AS-2.8 and AS-500 runs and the observations around the 800 hPa level. The tendency for a drying of the middle to low levels of the troposphere is well represented.

3.2 Impact on precipitating convection

In order to assess the impact on atmospheric latent instability as an ingredient of convection, Fig. 4a shows the spatially averaged temporal evolution of Convective Available Potential Energy (CAPE). Figure 4b represents the spatial averages of the hourly precipitation observations obtained from rain gauge measurements and the COSMO simulated precipitation at the nearest grid points. We can see three periods during the simulation period with existing CAPE, the first two coinciding with the diurnal cycle and the last one (starting at 24 September 2012, 00:00 UTC) induced by the arrival of the front. The changes seen in the spatially averaged CAPE between the CTRL and AS runs for the different model resolutions arise predominantly from changes in the moisture amount, given the weak impact of the assimilation on temperature. During the hours of the second CAPE maxima, on the 23 September 2012 at 18:00 UTC, the spatially averaged specific humidity was reduced about 0.25 g kg^{-1} for the simulations on the 7 km grid and 0.75 g kg^{-1} on the 2.8 km and 500 m grid simulations at the 850 hPa level (not shown). This drying caused a reduction in areal-mean CAPE of about 10 J Kg^{-1} in the simulations with the 7 km grid and 45 and 25 J Kg^{-1} in the simulations on the 2.8 km and 500 m grid respectively. During the precipitating hours the spatially averaged CAPE was reduced by the assimilation during the first hours of the event but was enhanced, most strongly in the 2.8 km and 500 m simulations, during the last hours. This happened as a result of a drying followed by wetting of the lowest tropospheric levels. These changes in CAPE affected the represented convection since for the CTRL runs, in this case study, less cells were triggered, the convection was found to be less organized and the intensity of the updrafts was weakened (not shown). The temporal evolution of precipitation for every grid spacing is consequently affected and lower precipitation totals for every model resolution are found as shown by Fig. 4b. On the 24 September 2012 at 04:00 UTC the hourly precipitation was decreased 1 mm in the 7 km and 500 m runs and 2 mm in the 2.8 km and 500 m runs. The structure and location of the precipitation maxima were likewise modified by the assimilation (not shown). Only the AS-2.8 run shows a late increase in precipitation as compared to its control homologue, this was due to the triggering of two isolated convective cells lasting for two hours over the north western part of A1, over the Alps, as a result of the increased CAPE over the area seen in Fig. 4a during the last hours of precipitation.

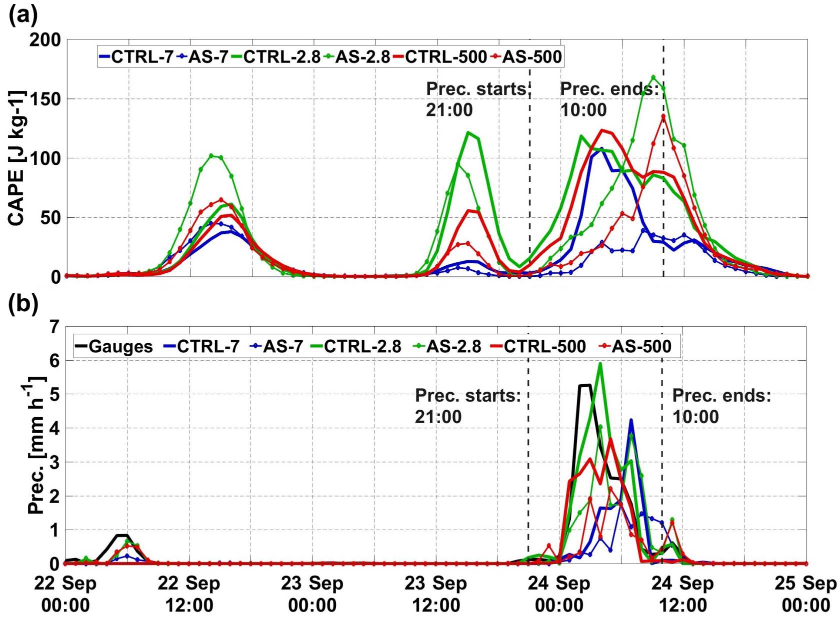

Figure 4. Spatial averages temporal evolution over area A1. **(a)** CAPE and **(b)** precipitation from rain gauges and COSMO at the nearest grid points.

4 Conclusions

The aim of this study is investigating the influence on heavy precipitation during HyMeX IOP 6 of an improved moisture distribution by assimilating GPS-ZTD across different horizontal resolutions (7 km, 2.8 km and 500 m). The NWP model COSMO was employed to simulate this HPE and results on the simulation of deep moist convection impacting the southern France region (A1) were shown.

The exclusive assimilation of GPS-ZTD data continuously every 10 min improved the representation of the amount, timing and distribution of IWV over the study region as demonstrated by the temporal evolution and the 24-hourly averaged spatial distribution of IWV for all three model resolutions. The impact on modelled convection of the humidity fields modified by the assimilation was strong for this case study as shown by the reduction of the updrafts intensity and of its organization and by the shift of the preferred spots for convection (not shown). However, relevant differences in the vertical profile of humidity still remain after the assimilation. Even though during the 6 h prior to storm initiation a tendency for a decrease in humidity below the 500 hPa level was well represented, the discrepancies in the stratification shown by the model and observations impede a clear improvement in the representation of heavy precipitation.

For this case study in southern France, the GPS-ZTD assimilation brought a decrease in IWV with the consequent decrease of atmospheric humidity, predominantly in heights below the 500 hPa level for every model horizontal resolution. As a consequence, the instability over the region was reduced as illustrated by CAPE, thus reducing the amount of convective precipitation over the area and inducing relevant differences in the precipitation location and structure.

In the future more case studies will be investigated to assess a more generalized response of modelled convection to the assimilation of GPS-ZTD.

Data availability. The model data employed in this study are property of the hosting research institution and are not publicly available. The GPS-derived datasets for ZTD and IWV are provided the LAboratoire de Recherche en Géodesie (LAREG) as part of L'Institut National de L'Information Géographique et Forestière (Bock and Bosser, 2014). The high-resolution satellite precipitation data set is provided by the Climate Prediction Center/National Centers for Environmental Prediction/National Weather Service/NOAA/U.S. Department of Commerce (CMORPH, 2017). The rain gauges and radiosonde data sets are provided by HyMeX and are made available for the HyMeX community.

Competing interests. The authors declare that they have no conflict of interest.

Acknowledgements. This research project is funded by the Bundesministerium für Bildung und Forschung (BMBF). It is a contribution to the HyMeX program supported by CNRS MISTRALS, ANR IODA-MED Grant ANR-11-BS56- 0005 and ANR REMEMBER Grant ANR-12-SENV-001.The authors thank the HyMeX database teams (ESPRI/IPSL and SEDOO/Observatoire Midi-Pyrenées) for their help in accessing the data. Finally, we thank Christoff Schraff (DWD) for his support in defining an

appropriate model set-up for the implementation of the GPS-ZTD data assimilation.

The article processing charges for this open-access publication were covered by a Research Centre of the Helmholtz Association.

Edited by: A. Cress
Reviewed by: three anonymous referees

References

Bevis, M., Businger, M., Herring, T. A., Rocken, C., Anthes, R. A., and Ware, R. H.: GPS meteorology: Remote sensing of atmospheric water vapor using the global positioning system, J. Geophys. Res., 97, 15787–15801, https://doi.org/10.1029/92JD01517, 1992.

Bock, O. and Bosser, P.: SOP reprocessed GPS delays and IWV, LAREG, https://doi.org/10.6096/MISTRALS-HyMeX.1280, 2014.

Bock, O., Bosser, P., Pacione, R., Nuret, M., Fourrié, N., and Parracho, A.: A high-quality reprocessed ground-based GPS dataset for atmospheric process studies, radiosonde and model evaluation, and reanalysis of HyMeX Special Observing Period, Q. J. Roy. Meteor. Soc., 142, 56–71, https://doi.org/10.1002/qj.2701, 2016.

Boniface, K., Ducrocq, V., Jaubert, G., Yan, X., Brousseau, P., Masson, F., Champollion, C., Chéry, J., and Doerflinger, E.: Impact of high-resolution data assimilation of GPS zenith delay on Mediterranean heavy rainfall forecasting, Ann. Geophys., 27, 2739–2753, https://doi.org/10.5194/angeo-27-2739-2009, 2009.

CMORPH: NOAA CPC Morphing Technique, Global Precipitation Analyses Version 1.0, Research Data Archive at the National Center for Atmospheric Research, Computational and Information Systems Laboratory, https://doi.org/10.5065/D60R9MF6, 2017.

Crook, N. A.: Sensitivity of moist convection forced by boundary layer processes to low-level thermodynamic fields, Mon. Weather Rev., 124, 1768–1785, 1996.

Davolio, S., Volonté, A., Manzato, A., Pucillo, A., Cicogna, A., and Ferrario, M. E.: Mechanisms producing different precipitation patterns over north-eastern Italy: insights from HyMeX-SOP1 and previous events, Q. J. Roy. Meteor. Soc., 142, 188–205, https://doi.org/10.1002/qj.2731, 2016.

Doms, G., Förstner, J., Heise, E., Herzog, H.-J., Mironov, D., Raschendorfer, M., Reinhardt, T., Ritter, B., Schrodin, R., Schulz, J.-P., and Vogel, G.: A description of the nonhydrostatic regional COSMO model, Part II: Physical parameterization, Deutscher Wetterdienst, Offenbach, Germany, 161 pp., available at: http://www.cosmo-model.org (last access: 2 June 2017), 2011.

Ducrocq, V., Braud, I., Davolio, S., Ferretti, R., Flamant, C., Jansa, A., Kalthoff, N., Richard, E., Taupier-Letage, I., Ayral, P., Belamari, S., Berne, A., Borga, M., Boudevillain, B., Bock, O., Boichard, J., Bouin, M., Bousquet, O., Bouvier, C., Chiggiato, J., Cimini, D., Corsmeier, U., Coppola, L., Cocquerez, P., Defer, E., Delanoë, J., Di Girolamo, P., Doerenbecher, A., Drobinski, P., Dufournet, Y., Fourrié, N., Gourley, J., Labatut, L., Lambert, D., Le Coz, J., Marzano, F., Molinié, G., Montani, A., Nord, G., Nuret, M., Ramage, K., Rison, B., Roussot, O., Said, F., Schwarzenboeck, A., Testor, P., Van, J., Vincendon, B., Aran, M., and Tamayo, J.: HyMeX-SOP1, the field campaign 1 dedicated to heavy precipitation and flash flooding in the north western Mediterranean, B. Am. Meteorol. Soc., 95, 1083–1100, https://doi.org/10.1175/BAMS-D-12-00244.1, 2014.

Hackenbruch, J., Schädler, G., and Schipper, J. W.: Added value of high-resolution regional climate simulations for regional impact studies, Meteorol. Z., 25, 291–304, https://doi.org/10.1127/metz/2016/0701, 2016.

Hally, A., Richard, E., and Ducrocq, V.: An ensemble study of HyMeX IOP6 and IOP7a: sensitivity to physical and initial and boundary condition uncertainties, Nat. Hazards Earth Syst. Sci., 14, 1071–1084, https://doi.org/10.5194/nhess-14-1071-2014, 2014.

Hastings, D. A., Dunbar, P. K., and Hittelman, A. M.: Assessing the global land one-km base elevation DEM, IAG Symp., 2000, 121, https://doi.org/10.1007/978-3-642-59742-8_16, 2000.

Lee, K.-O., Flamant, C., Ducrocq, V., Duffourg, F., Fourrié, N., and Davolio, S.: Convective initiation and maintenance processes of two back-building mesoscale convective systems leading to heavy precipitation events in Southern Italy during HyMeX IOP 13, Q. J. Roy. Meteor. Soc., 142, 2623–2635, https://doi.org/10.1002/qj.2851, 2016.

Schättler, U., Doms, G., and Schraff, C.: A description of the nonhydrostatic regional COSMO-model, Part VII: User's guide, Deutscher Wetterdienst, Offenbach, Germany, 200 pp., available at: http://www.cosmo-model.org (last access: 29 November 2016), 2013.

Schraff, C. and Hess, R.: A description of the nonhydrostatic regional COSMO-model, Part III: Data Assimilation, Deutscher Wetterdienst, Offenbach, Germany, 200 pp., available at: http://www.cosmo-model.org (last access: 2 June 2017), 2012.

Tiedtke, M.: A comprehensive mass flux scheme for cumulus parameterization in large-scale models, Mon. Weather Rev., 117, 1779–1800, 1989.